Journal of Power Sources 195 (2010) 6367–6372

Contents lists available at ScienceDirect

Journal of Power Sources

journal homepage: www.elsevier.com/locate/jpowsour

Carbon monoxide-fueled solid oxide fuel cell

Michael Homel[a], Turgut M. Gür[b,c,*], Joon Ho Koh[a], Anil V. Virkar[d]

[a] Materials and Systems Research, Inc., 5395 West 700 South, Salt Lake City, UT 84104, United States
[b] Direct Carbon Technologies, LLC, 525 University Avenue, Suite 1400, Palo Alto, CA 94301, United States
[c] Department of Materials Science and Engineering, Stanford University, Stanford, CA 94305, United States
[d] Department of Materials Science and Engineering, University of Utah, Salt Lake City, UT 84112, United States

ARTICLE INFO

Article history:
Received 11 March 2010
Received in revised form 6 April 2010
Accepted 7 April 2010
Available online 13 April 2010

Keywords:
CO fuel
CO oxidation
Power generation
Solid oxide fuel cell
Yttria stabilized zirconia
Ni cermet anode support

ABSTRACT

This study explored CO as a primary fuel in anode-supported solid oxide fuel cells (SOFCs) of both tubular and planar geometries. Tubular single cells with active areas of 24 cm^2 generated power up to 16 W. Open circuit voltages for various CO/CO_2 mixture compositions agreed well with the expected values. In flowing dry CO, power densities up to 0.67 W cm^{-2} were achieved at 1 A cm^{-2} and 850 °C. This performance compared well with 0.74 W cm^{-2} measured for pure H_2 in the same cell and under the same operating conditions. Performance stability of tubular cells was investigated by long-term testing in flowing CO during which no carbon deposition was observed. At a constant current of 9.96 A (or, 0.414 A cm^{-2}) power output remained unchanged over 375 h of continuous operation at 850 °C. In addition, a 50-cell planar SOFC stack was operated at 800 °C on 95% CO (balance CO_2), which generated 1176 W of total power at a power density of 224 mW cm^{-2}. The results demonstrate that CO is a viable primary fuel for SOFCs.

1. Introduction

Solid oxide fuel cells (SOFCs) offer fuel flexibility and high efficiency in converting chemical energy of fuel oxidation into electrical energy. They also provide high quality waste heat due to high operating temperatures ranging between 700 and 1000 °C. Hence, SOFCs are excellent candidates for combined heat and power generation applications.

Although there has been marked interest in direct oxidation of liquid and gaseous hydrocarbons in SOFCs [1–5], hydrogen remains the preferred fuel of choice for most studies and development efforts. There are several reasons that favor hydrogen. The attractive aspect of hydrogen as primary fuel is that environmentally friendly water is the only reaction product. Also, oxidation of hydrogen exhibits fast kinetics providing, in some cases, the high power densities of 1.7–1.9 W cm^{-2} at 800 °C reported in button cell measurements [6,7]. However, hydrogen is not a naturally occurring fuel and needs to be produced, mostly through steam reforming of natural gas or coal, and sometimes by electrolysis – processes that all require water.

In comparison to H_2, CO has not received much attention as a viable primary fuel for SOFCs. This may be partly due to its relatively higher anodic overvoltage [6,8–10] and accordingly slower oxidation kinetics for CO than for H_2 [11]. Nevertheless, power density as high as 0.7 W cm^{-2} at 800 °C has been demonstrated using pure CO as a fuel [6]. Also, the propensity of CO for carbon deposition (coking) at the anode is a major concern, since this can deactivate the anode and cause severe degradation in cell performance.

Energetics of CO and H_2 oxidation, calculated from thermochemical data [12] at an operating temperature of 850 °C, exhibit similar values for the standard Gibbs energy (i.e., −185 kJ mol^{-1} of CO_2 versus −186 kJ mol^{-1} of H_2O). Also, the enthalpy change for the CO oxidation reaction is slightly more exothermic than for the oxidation of H_2 (i.e., −282 kJ mol^{-1} of CO_2 versus −249 kJ mol^{-1} of H_2O).

There is considerable interest in the use of coal and coal-derived gases in SOFCs [13–21]. The objective of the present work is to determine the viability of CO as a practical fuel for SOFCs. However, this is not meant to be a mechanistic study of CO oxidation kinetics on SOFC anodes. More specifically, this work is motivated by and undertaken in the context of recent work in coal and carbon utilization in a solid oxide fuel cell arrangement coupled to a fluidized bed Boudouard gasifier [13–18].

The present paper demonstrates the use of CO as a primary fuel in SOFCs, where high power densities and stable performance over extended periods are achieved. These encouraging results obtained from single tubular cells and from a 50-cell planar stack warrant

* Corresponding author at: Department of Materials Science and Engineering, Stanford University, Stanford, CA 94305, United States. Tel.: +1 650 725 0107; fax: +1 650 725 8475.
E-mail address: turgut@stanford.edu (T.M. Gür).

0378-7753/$ – see front matter © 2010 Elsevier B.V. All rights reserved.
doi:10.1016/j.jpowsour.2010.04.020

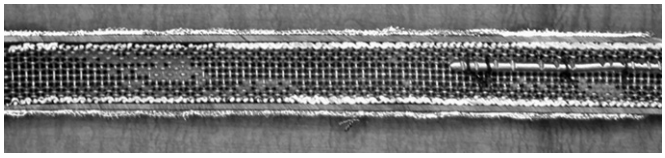

Fig. 1. Axial cross-section picture of a typical 1 cm OD tubular cell showing the mesh current collectors on the inside (anode) and outside (cathode) surfaces.

consideration of CO-fueled SOFCs for practical applications. However, it is not intended or envisioned that CO would be employed as a distributed fuel for stand-alone SOFCs, rather that the SOFC would be coupled with dry gasification of coal, biomass, or other solid carbonaceous fuels to create an efficient and integrated power generation system. A recent report [16] showed that this approach is a viable alternative to steam gasification or pulverized coal combustion processes and may offer significant advantages with regard to cost and efficiency, in particular where water supply is limited or CO_2 capture for sequestration becomes necessary. The operating principle and performance results of this process are described and discussed in detail elsewhere [13,17,18].

2. Experimental aspects

2.1. Tubular cell fabrication

The SOFC elements used for the single cell testing in this study were tubular in geometry using a Ni/YSZ anode-supported structure of 0.8–1.0 mm thickness and 9.4 mm diameter, coated with a 30 μm thick finely structured Ni/YSZ anode interlayer, and an 8–10 μm thick YSZ electrolyte membrane coated on the outer surface of the tube. The cathode comprises a 20 μm thick La–Sr–Mn–O (LSM)/YSZ composite catalytic interlayer deposited on the YSZ membrane, and a 25 μm thick porous La–Sr–Co–O (LSC) current collecting layer separated by a 10–15 μm thick compositionally graded LSM/LSC layer. The role of the interlayer is to serve as a chemical barrier to prevent a possible reaction between LSC and YSZ to form an insulating zirconate phase during primary firing of the cathode layers. After the cathode has been sintered, it is infiltrated with a solution of La, Sr, and Co salts. Upon firing, small particles of LSC are formed within the cathode structure. The purpose of introducing finely divided LSC is to improve cathode performance. The active geometric area of the cell was 24 cm^2. Silver and copper woven mesh was used for current collection on the cathode and anode surfaces, respectively. Fig. 1 shows an optical

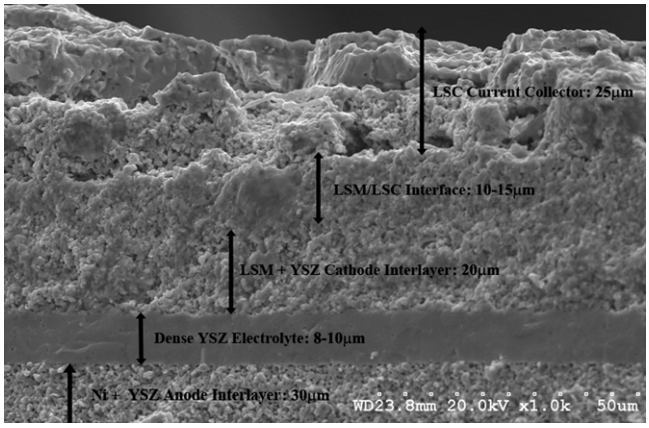

Fig. 2. Fracture cross-section scanning electron micrograph showing the anode interlayer, electrolyte, cathode interlayer, and cathode current collector of a typical tubular cell element used in this study.

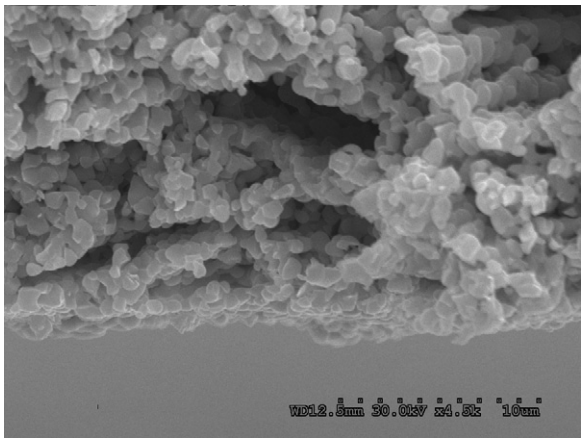

Fig. 3. Cross-section scanning electron micrograph showing the anode support of a typical tubular cell element used in this study.

picture of the cross-section of a typical tubular cell used in this study.

Fig. 2 shows a scanning electron micrograph (SEM) of a fractured cross-section of the typical tubular cell element. The compositions of the individual layers in the overall architecture of the tubular SOFC element are labeled in the picture. Similarly, the microstructural details of the outer surface of the fractured anode support are depicted in Fig. 3, indicating a grain size of about one micrometer and pore sizes on the order of several micrometers.

The tubular cells were tested with pure CO as well as with different CO/CO_2 gas mixtures as fuel in the temperature range from 800 to 900 °C. Current–voltage (I–V) characteristics of the cells were measured for constant fuel utilization values maintained by regulating the feed rate of the fuel by mass flow controllers. During these experiments, the cell voltage was usually kept above 0.65–0.7 V (versus air).

2.2. 50-Cell stack fabrication and testing

For the construction of a 1 kW-rated SOFC stack, fabrication of a planar cell geometry offered relative simplicity when compared to that of long tubular cells. Accordingly, the planar cell fabrication technology previously developed by Materials and Systems Research, Inc. (MSRI) was used to construct a 50-cell stack wherein the repeat unit comprised an anode-supported planar cell, stainless steel interconnect, compliant mica-glass gasket, and anode and cathode contact aids. The planar cells had similar architecture and microstructure with the tubular cells described above. They were fabricated on a tape-cast Ni-YSZ anode support (0.8–1.0 mm thick) with spray coated Ni-YSZ anode functional layer (~30 μm), spray coated YSZ electrolyte (8–10 μm), screen printed LSM-YSZ composite cathode functional layer (~30 μm), and screen printed LSC cathode current collector (~100 μm).

The typical active area of each cell (cathode area) was 100 cm^2. The repeat units were assembled between stainless steel endplates containing gas manifolds feeding air and fuel to the stack's internal flow channels as well as terminal connections for electrical current. Voltages were measured with leads attached to the metallic interconnects. Fig. 4 shows a photograph of the 50-cell stack, which measures 15.25 cm × 15.25 cm × 14.8 cm (height excluding endplates). The schematic structure of the planar stack repeat unit is shown in Fig. 5.

The stack was installed in an electrically heated test furnace with an external spring plate assembly to maintain a compressive force on the stack end plates. Brooks® 5850 series mass flow con-

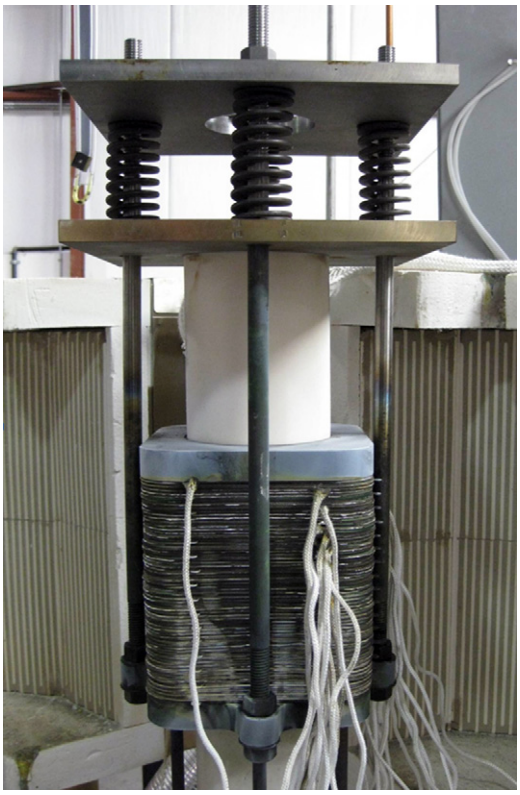

Fig. 4. Photograph of MSRI's 50-cell planar SOFC stack.

trollers were used to regulate anode and cathode inlet flow rates. Omegalux® electric gas heaters preheated inlet flows to ~550 °C (at the furnace inlet) to reduce thermal shock to the cells. Control and data acquisition were executed with a National Instruments Labview® system using a BNC-2110 analog I/O interface, SCB-68 shielded I/O connector block with a Keithley Integra® series 2700 multimeter DAQ. For electrochemical testing, the stack current was controlled using a Hewlett Packard 6060B system DC electronic load. Independent current measurements were made over a Grainger® 1 × 071 100A portable shunt resister. Furnace temperatures were monitored using Omega® *K*-type thermocouples located ~2 cm from the stack wall, i.e., within the hot zone of the furnace. Stack end plates were insulated to minimize heat loss through conduction and to reduce thermal gradients in the stack.

The stack was first heated under dilute H_2–N_2 gas to condition the glass seals and to reduce the NiO in the anode to nickel metal.

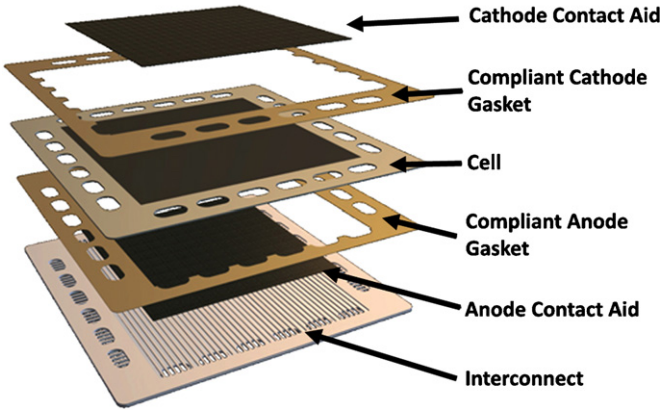

Fig. 5. Diagram of the planar stack repeat unit structure.

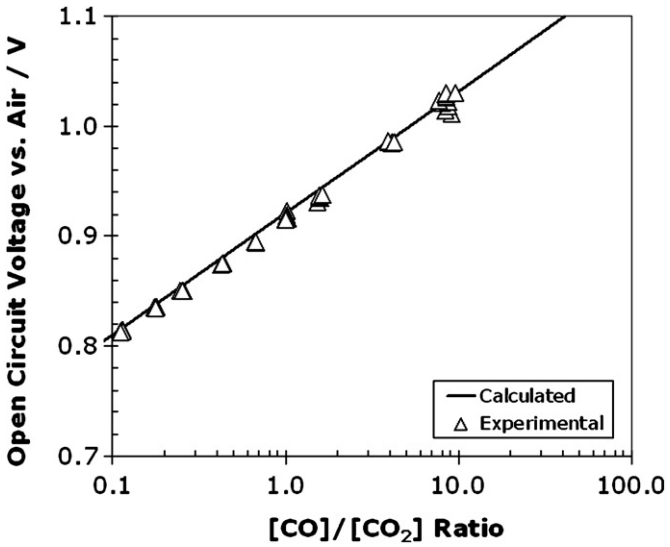

Fig. 6. Experimental and calculated values of the open circuit voltage versus air, for various CO/CO_2 compositions at 850 °C.

Baseline performance was measured on an H_2–N_2 mixture, and then the flow was switched to CO–CO_2 for performance testing. Polarization response was measured in a fixed-flow rate, current-controlled discharge.

3. Results and discussion

3.1. Open circuit voltage measurements

The open circuit voltages (OCV) using tubular cells at various CO/CO_2 ratios were measured at 850 °C and were compared with the theoretically expected values calculated from thermochemical data [5]. This is shown in Fig. 6. There is excellent agreement between the measured and calculated OCV values, indicating that equilibrium is readily established between the gas phase CO–CO_2 mixtures and the anode at this temperature.

3.2. Tubular single cell performance

The performance of tubular cells was benchmarked by operating them first on pure hydrogen for the same fuel utilization, U_f, and oxidant utilization, U_o, as was used with CO as the fuel. The constant utilization values during these experiments were maintained and monitored by regulating the mass flow controllers with a LabView control system.

There is significant variation in the performance results among anode supported cells reported in the literature, even where the materials composition and operating conditions are comparable. This may be due to differences in the microstructure among cells, interfacial and ohmic losses, or sheet resistance of the current collectors, as well as variation in experimental procedures that may result in different thermal or flow properties in the experimental setup.

To provide a reference baseline for assessing CO performance independent of experimental and microstructural differences, operating data were also obtained for H_2 using the same cells as were used for the CO tests. Fig. 7 shows the results of a benchmarking experiment at 850 °C on pure H_2 and pure CO measured on the same cell at a fuel utilization of 20%, and an oxidant utilization of 40%. The voltage–current–power (*V*–*I*–*P*) plot indicates a power density of 0.74 W cm^{-2} for H_2 and 0.67 W cm^{-2} for CO at a current density of 1 A cm^{-2}. The power density of 0.67 W cm^{-2}

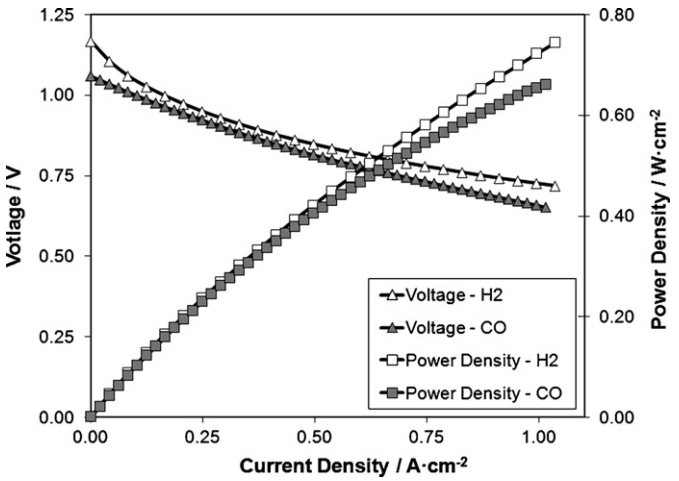

Fig. 7. Benchmarking test results with H_2 versus CO at 850 °C with equal fuel and oxidant utilization using the same cell element.

for CO at 850 °C compares reasonably well with the earlier result of Jiang and Virkar [6] who reported about 0.7 W cm^{-2} for CO oxidation at 800 °C on a button type anode-supported disc cell with an active cathode area of 1.1 cm^2.

The tubular anode-supported cells used in the present work with an active electrode area of 24 cm^2 were able to produce up to 16 W of power on CO as a fuel at a current density of 1 A cm^{-2}.

In earlier studies on button cells [6,8,11,22], it was observed that there was a significant difference in performance between H_2 and CO as fuels. This difference was attributed to differences in activation polarization associated with H_2 oxidation and CO oxidation since in button cell testing negligible losses occur in current collection. Thus, button cell tests more clearly distinguish between performance characteristics related to materials, fuel composition, temperature, etc. In the present work on tubular cells, the observed difference is much smaller. Given the fact that virtually identical materials were used in the earlier studies of Jiang and Virkar [6] and in the present work with the only difference being cell geometries (planar versus tubular), the observed apparent insensitivity of performance to fuel type must be related to geometric effects. Indeed, recent modeling by Virkar et al. [23] has shown that substantial losses are associated with current collection in tubular geometry which mask the effects of activation polarization between cells tested under different fuel types. This leads to apparent insensitivity to fuel type and temperature. Also, because of current collection losses, tubular cells tend to yield lower performance. Even in planar stacks, relative differences in performances with change of fuel (from H_2 to CO) are small due to greater current collection losses associated with the interconnect and contacts. The observation that excellent performance on a tubular cell was observed (0.67 W cm^{-2} at 850 °C) suggests that in the present work (Fig. 7) current collection losses were probably not limiting performance. Further testing of cell performance was conducted between 800 and 900 °C using 50:50 mole ratio CO–CO_2 and H_2–N_2 mixtures. The H_2–N_2 fuel mixture was again used for benchmarking purposes. These tests were conducted using a different cell for different fixed-flow rates equivalent to 20–50% fuel utilization at 0.5 A cm^{-2}. The results are presented in Fig. 8, which are generally lower than the performance values presented in Fig. 7. This difference in performance between individual cells may be related to possible cell-to-cell variations (microstructures, thicknesses of various layers) or to differences in effectiveness of current collection, which is related to contact between the electrodes and metallic current collection meshes.

A recent comparative study of CO and H_2 oxidation was reported on Ni/YZS and Cu/CeO_2/YSZ cermet anodes of 0.35 cm^2 active areas [24]. While the performance of H_2 on Ni/YSZ anode was clearly superior to CO oxidation (0.136 W cm^{-2} versus 0.073 W cm^{-2} at 700 °C, respectively), the Cu-ceria cermet cells showed almost identical performance for CO and H_2, both giving power density of about 0.305 W cm^{-2} at 700 °C. This result highlights the importance of the catalytic properties of the anode material [25], where ceria is known to be an effective oxidation catalyst for both CO and H_2. More interestingly, when Co is impregnated to make Cu–Co/ceria/YSZ bimetallic anode, the cell performance was greatly enhanced. The power densities for CO and H_2 fuels at 700 °C reported on Cu–Co/ceria/YSZ anode were 0.37 and 0.31 W cm^{-2}, respectively [24].

The power densities for CO oxidation on Ni/YSZ cermet anodes reported in the present study (and those reported by Jiang and Virkar [6]) are significantly larger than these literature values, and promise possibilities for further improvement in performance by developing better catalytic anodes for CO oxidation.

3.3. Electrical conversion efficiency

The electrical conversion efficiency, ε, for the cells is calculated from the expression, $\varepsilon = (U_f)\cdot(E/\mathrm{OCV})$, assuming that CO oxidation is Faradaic, and thus coulombic efficiency of the cell is 100%. Here, E is the operating voltage of the cell, OCV is the measured open circuit potential, which agreed well with the theoretically expected values (see Fig. 6) and U_f is the fuel utilization. The experimental data indicate that conversion efficiencies in excess of 50% can be achieved at practically significant power densities. Conversion efficiencies of 52% at 0.31 W cm^{-2}, of 55% at 0.22 W cm^{-2} and of 57% at 0.17 W cm^{-2} were obtained. These efficiency values are generally in good agreement with those reported earlier [13,17] and also with those predicted by a recent thermodynamic study [16].

3.4. Coking, or carbon deposition

Detectable levels of carbon deposition were not observed in the present work. The origin of carbon deposition at the anode is the CO disproportionation (i.e., reverse Boudouard) reaction:

$$2\mathrm{CO} = \mathrm{CO_2} + \mathrm{C} \quad (1)$$

In one atmosphere total pressure, $pCO + pCO_2 = 1$ (since pO_2 is proportional to $(pCO_2/pCO)^2$, and is negligibly small). As the tem-

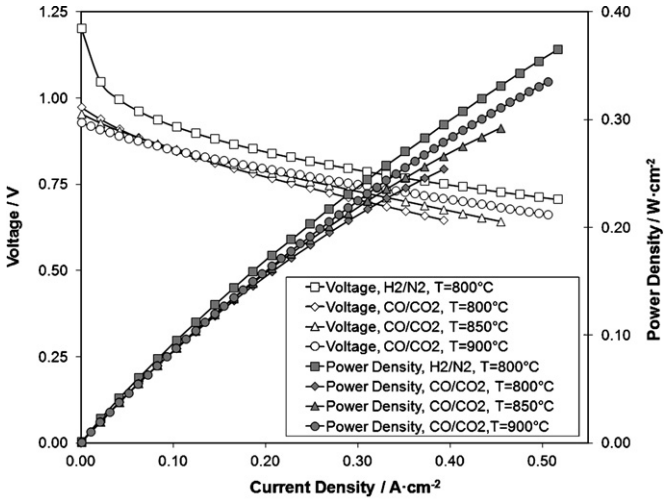

Fig. 8. *V–I–P* plot showing cell performance at different temperatures and fuel utilization, for 50:50 CO/CO_2 mixtures compared with 50:50 H_2/N_2 benchmarking experiments. Note the apparent insensitivity of performance to fuel type and temperature.

perature increases, the equilibrium shifts to the right in reaction (1). At 850 °C, carbon deposition is thermodynamically possible under open circuit conditions and where $pCO_2 < 0.05$ atm. In the present work, most of the experiments were conducted under nonzero current conditions. Thus, oxidation of CO at the anode by the reaction ($CO + O^{2-} \rightarrow CO_2 + 2e'$) continuously occurred. The CO_2 level in the anode gas was always maintained above the value required to prevent carbon deposition. Any initial carbon that was formed, possibly during open circuit conditions, was rapidly removed (oxidized) as soon as current was passed. Thus, during the actual operation of an SOFC on pure CO, no carbon deposition is expected. Several studies using *in situ* spectroscopic measurements [26–28] as well as pyrolytic carbon [29–31] have indeed shown that any deposited carbon is removed when current is passed through the cell.

3.5. Long-term stability of cell performance

Several tubular cells were tested under constant current in flowing 50:50 CO/CO_2 mixtures or pure CO for various durations ranging from tens of hours up to 375 h between 800 and 950 °C. Tests conducted at 850 °C or below showed no significant degradation in performance, while some degradation in cell performance was observed at temperatures above 900 °C. This performance degradation at 900 °C also occurred with H_2 as a fuel suggesting that degradation is not related to the choice of fuel. In these tests, one of the current collectors was silver mesh and it is quite possible that degradation at high temperatures is related to current collection, perhaps sintering of the silver mesh. For most cells, there was no obvious indication of degradation upon inspection, although partial delamination of the electrolyte layer from the anode was observed for a cell that was operated in pure hydrogen at 0.9 A cm^{-2} and was tested in various temperature steps between 800 and 900 °C over a period of 375 h.

The results of a long-term cell stability test on CO at 850 °C are shown in Fig. 9. The cell was initially held under open circuit in flowing pure CO gas, and then the long-term experiment commenced at a current density of 0.414 A cm^{-2}, or nearly 10 A of total current. After an initial voltage drop under a fixed current, the cell performance remained stable over the testing period of 375 h.

This initial drop shown in Fig. 9 has also been observed with other cells tested for long-term. The mechanism for this initial degradation has not yet been fully understood. It may be the result of a combination of effects including degradation of electrical contact at electrode-current collector interfaces, reduction in sealing efficacy, and chemical reaction between cell and stack components. Another possible explanation may be related to the

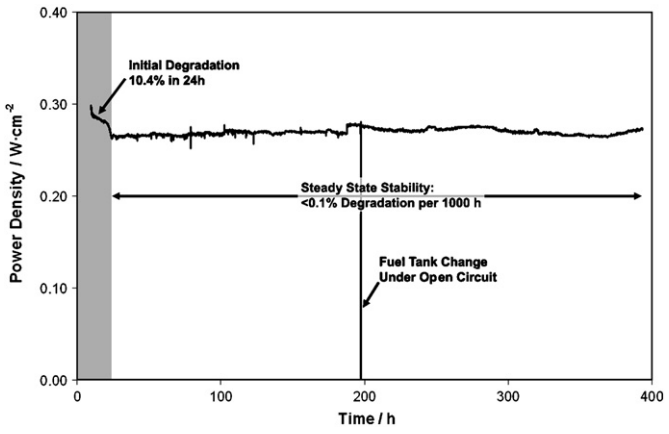

Fig. 9. Long-term cell performance result of a tubular SOFC element of 24 cm^2 active area, that is tested in flowing CO at 850 °C and under a constant current density of 0.414 A cm^{-2}. The data indicate stable cell power output over 375 h.

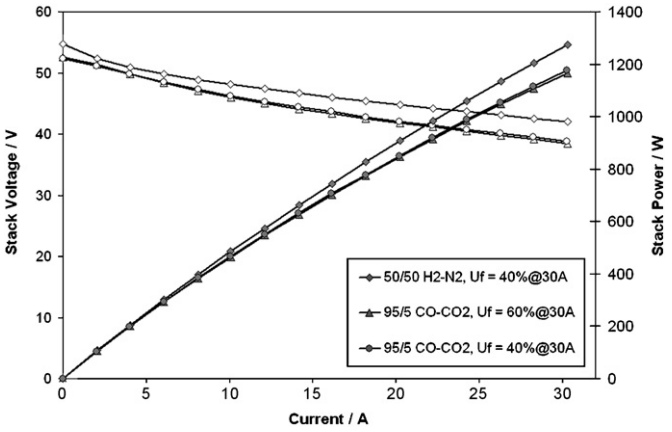

Fig. 10. Polarization response of a 50-cell planar SOFC stack tested on H_2–N_2 and CO–CO_2 at 800 °C.

removal of the residual surface carbon built up on the anode by oxygen that becomes available during discharge. As discussed above and verified by in situ Raman spectroscopy [26,28], graphitic carbon can build up on Ni anodes under open circuit conditions and may improve electrical conductivity of the anode. It was recently reported that carbon deposition during direct oxidation of hydrocarbons on Cu/ceria/YSZ anodes enhances anode conductivity and improves cell performance [32]. Since carbon is known to deposit preferentially on nickel relative to copper, this effect may be even more pronounced on Ni/YSZ anodes. After the commencement of long-term testing, carbon deposits are removed from the anode surface by oxidation. This may lower the anode conductivity and connectivity at the anode, resulting in a slightly lower power density for the same current, as reflected by the initial behavior in Fig. 9. From the amount of charge under the initial drop in Fig. 9, one can calculate the amount of carbon that would have been removed by oxidation. Accordingly, the amount of carbon removed was estimated to be of the order of 1 mole. Considering that the carbon deposit would be spread over and inside the porous anode of 24 cm^2 geometric area and with nearly 40% porosity, it is conceivable that the initial drop in the cell performance was due to the gradual oxidation and removal of the surface carbon that deposited under open circuit conditions before the long-term experiments were initiated. Further experimental investigation is warranted to substantiate this hypothesis.

3.6. 50-Cell planar SOFC stack performance

A 50-cell planar stack was installed in an electric furnace, and the performance was then measured at a furnace temperature of 785 °C. Tests were conducted under three flow conditions, using various fuels. (i) 50% H_2, 50% N_2 at a fixed-flow rate equivalent to 40% fuel utilization at 30 A; (ii) 95% CO, 5% CO_2 at a fixed-flow rate equivalent to 40% fuel utilization at 30 A; and (iii) 95% CO, 5% CO_2 at a fixed-flow rate equivalent to 60% fuel utilization at 30 A. For all data sets, the airflow was held at a fixed rate equivalent to 40% oxidant utilization at 30 A. The results are shown in Fig. 10. Note that the fuel and oxidant utilizations given in the inset correspond to an electrical current of 30 A, but at values other than 30 A, both the fuel and oxidant utilizations differ from these values.

The stack produced 1176 and 1165 W on CO/CO_2, at a fuel utilization of 40% and 60%, respectively, and produced 1275 W on H_2/N_2 at 40% fuel utilization. While small single button cells consistently showed larger variation between CO-fueled and H_2-fueled performance [6,10,11,22], the results of this test suggests that the effects causing these differences are largely masked in larger SOFC modules by other losses. Since most of these other losses are gen-

erally unavoidable, the relative performance differences between H_2-fueled and CO-fueled practical SOFC systems are modest. The present results provide further support for CO as a potential fuel for SOFC.

To the authors' knowledge, this 50-cell demonstration represents the first test reported in the literature for large scale testing of an SOFC stack fueled exclusively by dry CO. This testing provides encouraging results that warrant further investigation and development of SOFC anodes and structures that enhance CO oxidation.

The tubular and planar cells used in this study were both anode-supported with the same materials composition and cell structure. Some variation in the electrode microstructure exists due to differences in fabrication methods since the planar cells comprise a tape-cast anode support with spray-coated electrolyte and screen printed cathode, whereas the tubular cells comprise a slip-cast anode support with dip-coated electrolyte, and hand-painted cathode layers.

Data for both tubular and planar cell geometries are presented not only to show the effects of such microstructural differences, but also to demonstrate the viability of CO as primary fuel in a relevant platform for scalable power generation. As such, it is important to demonstrate not only performance under idealized single cell testing conditions, but also in a multi-cell assembly where temperature variation, non-uniform flow distribution, current collector losses, and chemical reaction between reactants and stack components (cell, interconnect, contact aides, gaskets) may present significant challenges. Furthermore it is important to note that differences in performance at a single cell level may be masked in a stack level test. This relates directly to the motivation for a CO-fueled stack demonstration as it relates to a coupled SOFC – fluidized bed Boudouard gasifier. Since the difference in cell performance between a CO-fueled and H_2-fueled stack is small, the relative economics of the two processes will be dictated by the cost and availability of the fuel sources, rather than by small differences in conversion efficiencies.

4. Summary

This study demonstrates the potential and viability of CO as a primary fuel for SOFCs. Pure, dry CO and CO/CO_2 mixtures were employed in Ni/YSZ anode-supported tubular SOFCs with active areas of 24 cm^2. Power densities up to 0.67 $W\,cm^{-2}$ that were obtained in pure CO at 850 °C translate into 16 W of power per cell. The cells also demonstrated stable performance for up to 375 h of continuous operation at 0.414 $A\,cm^{-2}$. No carbon deposition was observed on the anodes after the tests, in agreement with recent studies of *in situ* Raman on SOFCs. Also, a 50-cell planar SOFC stack was tested with CO and produced 1176 W of power at 800 °C. These results represent practical scale stack tests employing dry CO exclusively as the primary fuel. The long-term stability and high performance of cells in CO fuel warrant further exploration and consideration of CO as a primary fuel and development of catalytic anodes specifically for CO oxidation.

Acknowledgements

This material is based upon work supported in part by the Department of Energy National Energy Technology Laboratory under Award Number DE-NT0004395, and in part under NAVY contract No. N666 04-08-C-1957. The authors also acknowledge partial financial support from Direct Carbon Technologies, LLC.

References

[1] S. Park, J.M. Vohs, R.J. Gorte, Nature 404 (2000) 265.
[2] H. Kim, S. Park, J.M. Vohs, R.J. Gorte, J. Electrochem. Soc. 148 (7) (2001) A693.
[3] S. McIntosh, R.J. Gorte, Chem. Rev. 104 (10) (2004) 4845.
[4] Z. Zhan, S.A. Barnett, Science 308 (2005) 844.
[5] M. Mogensen, K. Kammer, Annu. Rev. Mater. Res. 33 (2003) 321.
[6] Y. Jiang, A.V. Virkar, J. Electrochem. Soc. 150 (7) (2003) A942.
[7] S. DeSouza, S.J. Visco, L.C. DeJonghe, Solid State Ionics 98 (1997) 57.
[8] T.H. Etsell, S.N. Flengas, J. Electrochem. Soc. 118 (12) (1971) 1890.
[9] S.V. Karpachov, A.T. Filyaev, S.F. Palguyev, Electrochim. Acta 9 (1964) 1681.
[10] H. Yakabe, M. Hishinuma, M. Uratani, Y. Matsuzaki, I. Yasuda, J. Power Sources 86 (2000) 423.
[11] P. Holtappels, L.G.J. de Haart, U. Stimming, I.C. Vinke, M. Mogensen, J. Appl. Electrochem. 29 (1999) 561.
[12] I. Barin, Thermochemical Data of Pure Substances, 3rd edition, VCH, Weinheim, Germany, 1995.
[13] A.C. Lee, S. Li, R.E. Mitchell, T.M. Gür, Electrochem. Solid State Lett. 11 (2) (2008) B20.
[14] S. Li, A.C. Lee, R.E. Mitchell, T.M. Gür, Solid State Ionics 179 (2008) 1549.
[15] A.C. Lee, R.E. Mitchell, T.M. Gür, AIChE J. 55 (4) (2009) 983.
[16] A.C. Lee, R.E. Mitchell, T.M. Gür, J. Power Sources 194 (2009) 774.
[17] T.M. Gür, M. Homel, A.V. Virkar, J. Power Sources 195 (2010) 1085.
[18] T.M. Gür, ECS Trans. 25 (2) (2009) 1099.
[19] D.H. Archer, R.L. Zahradnik, Chem. Eng. Progr. Symp. Series 63 (1967) 55.
[20] M.C. Williams, J.P. Strakey, W.A. Surdoval, J. Power Sources 143 (2005) 191.
[21] M.C. Williams, J.P. Strakey, W.A. Surdoval, J. Power Sources 159 (2006) 1241.
[22] A.M. Sukeshini, B. Habibzadeh, B.P. Becker, C.A. Stoltz, B.W. Eichhorn, G.S. Jackson, J. Electrochem. Soc. 153 (4) (2006) A705.
[23] A.V. Virkar, F.F. Lange, M.A. Homel, J. Power Sources 195 (2010) 4816.
[24] O. Costa-Nunes, R.J. Gorte, J.M. Vohs, J. Power Sources 141 (2005) 241.
[25] A. Atkinson, S. Barnett, R.J. Gorte, J.T.S. Irvine, A.J. McEvoy, M. Mogensen, S.C. Singhal, J. Vohs, Nat. Mater. 3 (2004) 17.
[26] M.B. Pomfret, J.C. Owrutsky, R.A. Walker, J. Phys. Chem. B 110 (35) (2006) 17305.
[27] Z. Cheng, M. Liu, Solid State Ionics 178 (13/14) (2007) 925.
[28] M.B. Pomfret, J.C. Owrutsky, R.A. Walker, Anal. Chem. 79 (2007) 2367.
[29] M. Ihara, S. Hagesawa, J. Electrochem. Soc. 153 (8) (2006) A1544.
[30] M. Ihara, K. Matsuda, H. Sato, C. Yokoyama, Solid State Ionics 175 (2004) 51.
[31] X.-Y. Zhao, Q. Yao, S.-Q. Li, N.-S. Cai, J. Power Sources 185 (1) (2008) 104.
[32] S. McIntosh, J.M. Vohs, R.J. Gorte, J. Electrochem. Soc. 150 (4) (2003) A470.